

## SPUTTER DEPOSITION AND CHARACTERIZATION OF $\text{Cd}_2\text{SnO}_4$ FILMS

G. HAACKE, W. E. MEALMAKER AND L. A. SIEGEL

*Chemical Research Division, American Cyanamid Company, Stamford, Conn. 06904 (U.S.A.)*

(Received April 23, 1978; accepted May 1, 1978)

Cadmium stannate ( $\text{Cd}_2\text{SnO}_4$ ) films were prepared by r.f. sputtering from  $\text{Cd}_2\text{SnO}_4$  powder or cadmium–tin alloy targets. The films were transparent to visible light and electrically conductive. Their optical transmission and electrical conductivity depended on the sputtering conditions, the post-deposition heat treatment and the presence of secondary phases (mainly  $\text{CdSnO}_3$  and  $\text{CdO}$ ). The influence of deposition parameters and heat treatment on the film composition and electrical and optical properties is discussed.

### 1. INTRODUCTION

The semiconducting compound  $\text{Cd}_2\text{SnO}_4$  is a promising candidate for transparent electrode applications<sup>1</sup>. The figures of merit characterizing the transparent conductor performance of sputtered films<sup>2</sup> are high as a result of high electrical conductivities and good visible transparency. It seems possible that still better transparent electrode properties can be obtained in  $\text{Cd}_2\text{SnO}_4$  but further progress may largely depend on a thorough understanding of the influence of film structure and composition on the electrical conductivity and optical absorption.

Improved film characterization is also needed to determine reliably the intrinsic electrical and optical constants and to explain several unexpected observations associated with the sputtered coatings. For example, the fundamental optical absorption edge shows an unusually large shift to shorter wavelengths with increasing electrical conductivity<sup>3</sup>. Furthermore, post-deposition heat treatment not only raises the free-electron concentration appreciably but also increases the Hall mobilities<sup>4</sup>.

We prepared cadmium stannate films by different sputtering techniques including reactive sputtering and bias sputtering and we determined their electrical conductivities, Hall effects, optical transmissions and structural properties. The experimental data allow us to offer tentative interpretations of earlier observations<sup>3,4</sup> but more work is necessary before the properties of these films are completely understood.

### 2. EXPERIMENTAL TECHNIQUES

#### 2.1. Sample preparation

All samples were prepared in a 45 cm vacuum chamber by sputtering from target plates 12.5 cm in diameter. The pressure  $((5\text{--}10) \times 10^{-3}$  Torr) was monitored

with a Varian dual-range ion gauge controller and was regulated by a servo-driven valve assembly in conjunction with a Granville-Phillips automatic pressure controller. The plasma gas consisted in most cases of ultrahigh purity oxygen. Argon-oxygen mixtures or air were also used but the highest electrical conductivities (after heat treatment) invariably occurred in samples sputtered in pure oxygen. Sputtering in pure argon led to the formation of Cd-Sn metal films because the oxide targets were rapidly reduced. This effect has also been observed in other oxide materials<sup>5</sup>.

The plasma discharge was maintained by r.f. power delivered to the target from an r.f. generator (MRC model S-3007, 13.6 MHz) via an impedance-matching network. Depending on the mechanical stability of the target, up to 1.2 kW r.f. power could be used for film deposition. Metal targets sustained exposure to 1.2 kW without difficulty. Hot-pressed ceramic targets developed cracks above 700 W while targets prepared by powder settling (see below) were useful only below 200–300 W.

The water-cooled target plates were mounted face down in the top plate of the sputter system and could be easily exchanged. The substrates rested under the target (6 cm target-substrate distance) on a stainless steel bifilar resistance heater (7.5 cm in diameter) which allowed us to maintain the substrates at temperatures up to 750 °C during deposition (monitored by a thermocouple near the heater-substrate interface). Substrate heating could be accomplished more economically by the r.f. plasma but without being able to control the deposition rate and substrate temperature independently.

Before deposition all the substrates were cleaned in an ultrasonic bath consisting of 10 vol.% ammonium hydroxide, 10 vol.% Aquasol cleaning solution (L & R Manufacturing Company, Kearney, New Jersey) and 80 vol.% deionized water. After removal from the bath the substrates were thoroughly rinsed first with distilled water and then with Baker analyzed-reagent-grade acetone and were finally dried with a heat gun.

Most of the sputtered films received a post-deposition heat treatment in which the samples were heated on an alumina support inside a Vycor tube (6 cm in diameter) in a gas stream. During preliminary experiments hydrogen was found to reduce the Cd<sub>2</sub>SnO<sub>4</sub> completely at temperatures above 400 °C. The improvements in the transparent electrode properties achieved below 400 °C in hydrogen were significantly smaller than those obtained at higher temperatures in an inert atmosphere; heat treatment in argon or nitrogen could be performed up to approximately 700 °C before film deterioration became apparent. Argon was selected as the standard atmosphere for convenience. Later investigations revealed that the presence of cadmium sulfide during the post-deposition heat treatment led to higher electrical conductivities than when argon alone was used and extended short wavelength transmissions. These experiments were carried out in flowing argon (as above) but the samples were covered with a thin layer of CdS powder (this experimental situation will be referred to as Ar-CdS conditions). The CdS powder had to be free of adsorbed moisture and oxygen to prevent stains from developing in the cadmium stannate films.

## 2.2. Substrate materials

Cadmium stannate films can be sputter coated onto many different materials.

Silica is the most convenient especially when heat treatment is involved. Its major disadvantages are cost and a low coefficient of thermal expansion  $\beta$ . Although the low  $\beta$  provides a high tolerance to thermal shock, it is also responsible for the formation of fine hairline cracks in the  $\text{Cd}_2\text{SnO}_4$  whenever the film thickness exceeds certain values<sup>6</sup>. This effect is caused by thermal stresses resulting from the difference in coefficients of expansion across the substrate-film interface. Films sputtered onto vitreous silica slides (ESCO Products, CO grade) were found to develop hairline cracks when their thickness was larger than about  $2 \times 10^{-4}$  cm. Glasses with values of  $\beta$  exceeding  $4 \times 10^{-6} \text{ }^\circ\text{C}^{-1}$  did not induce cracking in the sputtered  $\text{Cd}_2\text{SnO}_4$  coatings and of these Corning 7059 was the most suitable in view of its high softening point (840  $^\circ\text{C}$ ).

Other substrate materials onto which we sputter coated cadmium stannate included single-crystal sapphire, spinel, quartz and silicon. Polycarbonate plastics and acrylics can be coated if thin metal oxide interlayers are deposited first<sup>7</sup>. In the case of single-crystal silicon substrates it is interesting to note that the condition of the substrate surface considerably influences the rate of deposition. On chemically etched wafers a deposition rate of  $300 \text{ \AA min}^{-1}$  was attained at 800 W r.f. power. For the same power input the deposition rate increased to  $400 \text{ \AA min}^{-1}$  when the wafer surface was only mechanically lapped.

### 2.3. Target preparation

Three types of targets were used: hot-pressed ceramic targets, metal alloy targets and targets made by a settling technique. For the ceramic targets  $\text{Cd}_2\text{SnO}_4$  powder was synthesized by firing stoichiometric proportions of CdO (Fisher C-16) and  $\text{SnO}_2$  (Baker 3975) powders in alumina crucibles for 6 h at 1050  $^\circ\text{C}$  in air. After furnace cooling, the product was bright yellow and according to X-ray diffraction (XRD) analysis consisted of the orthorhombic  $\text{Cd}_2\text{SnO}_4$  phase<sup>8</sup> with no secondary phases detectable. The  $\text{Cd}_2\text{SnO}_4$  powder was hot pressed into discs 6 mm thick (12.5 cm in diameter) and was perma-bonded to stainless steel backing plates by Materials Research Corporation (Orangeburg, New York).

Cadmium-tin alloy plates (12.5 cm in diameter, 6 mm thick) were purchased from Haselden Company (San Jose, California) and were bonded to backing plates with conductive silver epoxy (Dynaloy 326). The starting materials for the cadmium-tin alloy were 99.999% pure cadmium and tin.

Frequently the need arose for targets with an off-stoichiometric composition or that contained doping materials of varying concentrations. To avoid making expensive ceramic targets for each new composition an economical fabrication technique was developed. The preparation was started by thoroughly grinding the doped cadmium stannate powder under methanol using a mortar and pestle and by occasionally decanting and collecting the  $\text{Cd}_2\text{SnO}_4$  suspension. The collected suspension was poured over a target backing plate until a layer 3 cm deep covered its top surface. The backing plate, previously sputter coated with a layer of  $\text{Cd}_2\text{SnO}_4$  1  $\mu\text{m}$  thick, sat in a Buchner funnel which had its spout closed by a rubber hose and a hose clamp. The suspended  $\text{Cd}_2\text{SnO}_4$  settled onto the target plate within 10–15 h after which time the methanol could be slowly drained off. The  $\text{Cd}_2\text{SnO}_4$  layers formed by this method were approximately 1 mm thick; they were mechanically

stable and adhered well enough to the backing plate to be useful for 5–10 depositions at low power levels.

#### 2.4. *Sputter modes*

Most of the depositions were carried out with a floating substrate potential ( $\pm 10$  V or less). When it became apparent that the films sputtered in this mode were not single phase, d.c. bias sputtering<sup>9</sup> was investigated to see whether substrate bias would lead to single-phase films<sup>10</sup>. Negative d.c. potentials up to  $-200$  V were applied to the substrates from a d.c. power supply through an impedance network. Special shielding was installed to prevent back-sputtering from parts other than the growing film. Electrical contact to the substrate surface was made by a shielded gold clip pressing against a strip electrode of conductive cadmium stannate 2 mm wide deposited onto the substrate prior to the bias sputtering. The effectiveness of the bias potential could be observed visually by the formation of a dark space in front of the substrate.

Reactive sputtering from the Cd–Sn alloy targets was investigated with a view to improving the economics of the film preparation. Metal alloy targets are less expensive than ceramic  $\text{Cd}_2\text{SnO}_4$  targets, especially when large target diameters are required. The superior mechanical stability of metal targets would be important in a production environment and would also facilitate much higher deposition rates. The deposition conditions for films of high conductivity were identical for sputtering from metal or ceramic targets (pure oxygen plasma,  $(5\text{--}10) \times 10^{-3}$  Torr).

#### 2.5. *Measurement techniques*

Electrical sheet resistances were measured either with a four-point probe or by the standard two-point method using indium-soldered contacts. Hall measurements were carried out in the three-probe configuration in magnetic fields up to 19.3 kOe.

The film thickness was determined from the position of the interference maxima in optical transmission curves and from the index of refraction<sup>3</sup>. Cross checks were made in films which had a well-defined step by measuring the step height with either a Sloan Angstrometer or a Sloan Dektak. In several samples the film thickness obtained by step height and optical transmission measurements was also checked by observing a fracture plane edge-on with a scanning electron microscope. The thickness values from all three methods agreed to within  $\pm 8\%$ .

Optical transmission in the visible and infrared was measured using a Cary 14 and a Beckman IR 4240 spectrophotometer with blank substrates positioned in the reference beam. Luminous transmittances were determined with a General Electric Hardy spectrophotometer without substrate blanks in the reference beam.

The structure, phase composition and cadmium:tin ratios of the films were determined using a computerized X-ray diffractometer (Rigaku) and an Ortec energy dispersive X-ray fluorescence spectrometer. The Ortec instrument was calibrated by using thin layers of  $\text{Cd}_2\text{SnO}_4$  powders whose Cd:Sn ratios were determined quantitatively by atomic absorption.

### 3. FILM STRUCTURE AND COMPOSITION

When cadmium stannate is sputtered onto substrates kept at or near room

temperature the resulting films do not show X-ray diffraction lines<sup>3</sup>. It is difficult to establish relationships between the electrical and optical properties and the composition for these films since they can be characterized only by their Cd:Sn ratio which in most cases is close to 2. To obtain coatings with well-developed X-ray diffraction patterns, the substrates have to be maintained at elevated temperatures during deposition. The minimum substrate temperature needed for film crystallization depends on the substrate surface. Amorphous surfaces such as glass or vitreous silica require approximately 400–500 °C but we found that crystalline films grew on single-crystal spinel substrates (Union Carbide), for example, at temperatures as low as 150 °C. Epitaxial growth of single-crystal films has not been achieved however.

The crystal structures of the sputtered cadmium stannate films, whether they were prepared from the  $\text{Cd}_2\text{SnO}_4$  powder or the Cd–Sn alloy targets, did not have orthorhombic symmetry but were cubic spinel<sup>11</sup>. Depending on the deposition conditions and the composition of the target surface, the X-ray patterns also contained CdO and  $\text{CdSnO}_3$  lines. For example, coatings prepared from the  $\text{Cd}_2\text{SnO}_4$  ceramic targets under conditions of poor r.f. tuning (off-resonance) consisted of the major  $\text{Cd}_2\text{SnO}_4$  phase and small concentrations of CdO and  $\text{CdSnO}_3$ . A typical pattern for these films is shown schematically in Fig. 1. The intensity and number of the spinel lines depend on crystallite orientation. The  $\text{CdSnO}_3$  line does not correspond to the pattern of the bulk material and was identified from the X-ray diffraction pattern of a film sputtered from a  $\text{CdSnO}_3$  target.

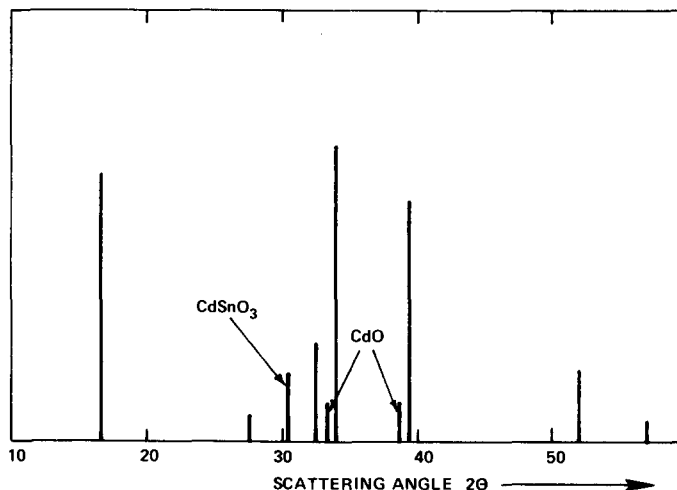


Fig. 1. The positions of X-ray diffraction lines for a  $\text{Cd}_2\text{SnO}_4$  film prepared by r.f. sputtering (Cu  $K\alpha$  radiation).

The  $\text{CdSnO}_3$  phase could be avoided by sputtering from  $\text{Cd}_2\text{SnO}_4$  targets and by keeping the r.f. system tuned at full resonance and minimum reflected power; however, under these conditions cadmium oxide still formed in the films. In many samples the CdO phase was indicated only by the 2.32 Å CdO line forming a shoulder on the 2.29 Å  $\text{Cd}_2\text{SnO}_4$  spinel line (Fig. 2).

### 3.1. Bias sputtering from $\text{Cd}_2\text{SnO}_4$ targets

Cadmium stannate films free from CdO could be prepared by applying a negative d.c. bias voltage to the substrate during deposition. When the system was tuned so that CdO was noticeable only by the 2.32 Å shoulder, an increasing bias reduced this shoulder until it disappeared at approximately  $-200$  V (Fig. 2).

Although cadmium oxide disappeared with increasing d.c. bias, the  $\text{CdSnO}_3$  phase developed simultaneously. Since the  $\text{Cd}_2\text{SnO}_4$  and  $\text{CdSnO}_3$  X-ray lines were well separated the increase of  $\text{CdSnO}_3$  with bias voltage could be derived semiquantitatively from the X-ray patterns. As a relative measure of the  $\text{CdSnO}_3:\text{Cd}_2\text{SnO}_4$  ratio the peak areas of the 2.29 Å  $\text{Cd}_2\text{SnO}_4$  and 2.96 Å  $\text{CdSnO}_3$  lines were determined. This approach is justified by the observation that the X-ray patterns of bias-sputtered films contained only the 2.96 Å line for  $\text{CdSnO}_3$  and apart from the dominant 2.29 Å line only one or two weak  $\text{Cd}_2\text{SnO}_4$  lines. The dependence of the  $\text{CdSnO}_3:\text{Cd}_2\text{SnO}_4$  ratio, as defined above, on bias voltage is shown in Fig. 3. Starting with  $\text{CdSnO}_3$ -free films at floating substrate potential, the  $\text{CdSnO}_3:\text{Cd}_2\text{SnO}_4$  ratio increases exponentially until  $-200$  V bias (the highest voltage applicable in our system). Assuming a continuation of the exponential increase beyond  $-200$  V, the bias-sputtered films should be nearly free of  $\text{Cd}_2\text{SnO}_4$  at  $-400$  V.

### 3.2. Reactive sputtering

Sputtering from metal alloy targets often removes one of the target components at a higher rate than the other(s), resulting in a compositional change at the target surface<sup>12</sup>. Under constant deposition conditions the target surface eventually acquires a new equilibrium composition which determines the composition of the growing film. We observed this effect during the preparation of cadmium stannate films from the Cd-Sn alloy targets (Cd:Sn = 2:1 at. %). Initially the sputter rate of cadmium was larger than that of tin. Consequently, the first coatings sputtered from a new target were rich in CdO and had poor transparent electrode properties. With increasing sputter time the target surface became cadmium deficient and the CdO content of the films decreased. At equilibrium enough cadmium had been lost from the target surface for the films to contain  $\text{CdSnO}_3$ .

Figure 4 shows the changes that occurred in the film composition with increasing target usage. The experiments started with a virgin target as received from the manufacturer. An initial sputtering for 30 min at low r.f. power (80 W) against the shutter preceded the series of sample preparations which were carried out under identical conditions: 20 min deposition time at 950 W r.f. power in pure oxygen ( $8.5 \times 10^{-3}$  Torr). The resulting films were heat treated for 20 min at 650 °C under Ar-CdS conditions and were then analyzed by energy dispersive X-ray fluorescence spectroscopy (EDX) (Cd:Sn ratio) and by XRD ( $\text{CdO}:\text{Cd}_2\text{SnO}_4$  and  $\text{CdSnO}_3:\text{Cd}_2\text{SnO}_4$  ratios). The  $\text{CdSnO}_3:\text{Cd}_2\text{SnO}_4$  ratios were determined from the X-ray diffraction peak areas as described above while a rough estimate of the  $\text{CdO}:\text{Cd}_2\text{SnO}_4$  ratios was obtained from the peak heights of the dominant 2.29 Å  $\text{Cd}_2\text{SnO}_4$  line and the 2.32 Å CdO line. Reliable peak areas could not be calculated for these two lines because of partial overlap. In Fig. 4 the compositional parameters are plotted against the accumulated sputter time. Under the given set of experimental conditions target-surface equilibrium was reached after approxi-

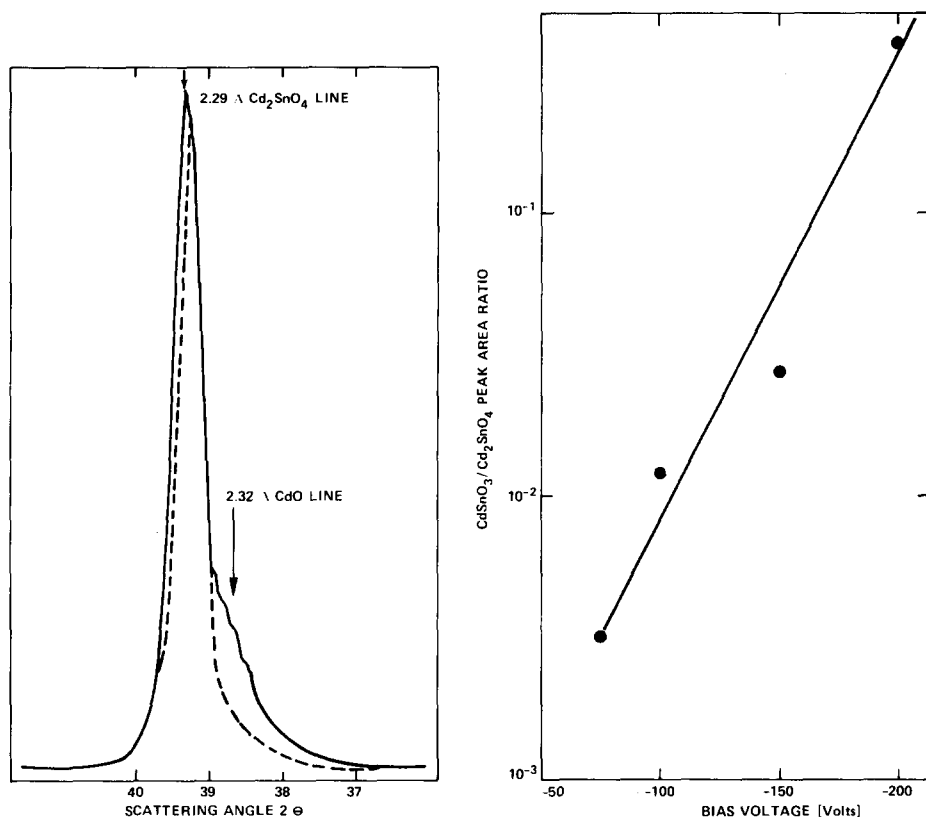


Fig. 2. The dominant X-ray diffraction line of two  $\text{Cd}_2\text{SnO}_4$  films sputtered with and without substrate bias: —, floating potential, sample A; ---, -200 V bias, sample A after a 750 °C anneal.

Fig. 3. The ratio of the peak areas of the 2.96 Å  $\text{CdSnO}_3$  and 2.29 Å  $\text{Cd}_2\text{SnO}_4$  X-ray lines as a function of d.c. bias voltage for films sputtered from a  $\text{Cd}_2\text{SnO}_4$  ceramic target.

mately 250 min. From the measured film thicknesses ( $\approx 0.8 \mu\text{m}$ ) it was estimated that roughly  $10 \mu\text{m}$  of the target surface was removed during this time. Assuming that the Cd:Sn ratio of the sample films at equilibrium reflects the composition of the target surface, Fig. 4 shows that the target surface lost 11% cadmium before it stabilized at a Cd:Sn ratio of 1.78. To achieve an equilibrium stoichiometry of  $2\text{Cd}:1\text{Sn}$  the alloy target must contain excess cadmium.

### 3.3. Heat treatment

Cadmium stannate films prepared either by reactive sputtering or by sputtering from a  $\text{Cd}_2\text{SnO}_4$  target have unimpressive transparent electrode properties. The samples are brownish because of an apparent band gap of approximately 2.1 eV and their electrical conductivities are low. Post-deposition heat treatment shifts the optical absorption edge towards higher energies and increases the electrical conductivity. To uncover the mechanism(s) responsible for these changes we determined the film structure and composition as a function of heat treatment. The experiments were carried out with eight films prepared

simultaneously by reactive sputtering and heat treated for 20 min at different temperatures  $T_H$  under Ar–CdS conditions. The Cd:Sn ratios determined by EDX are shown in Fig. 5 as a function of  $T_H$ . There is no significant change in the Cd:Sn ratio until 700 °C, after which it drops substantially. The electrical sheet resistance decreases with  $T_H$ , reaches its minimum value between 650 and 670 °C and then rises sharply.

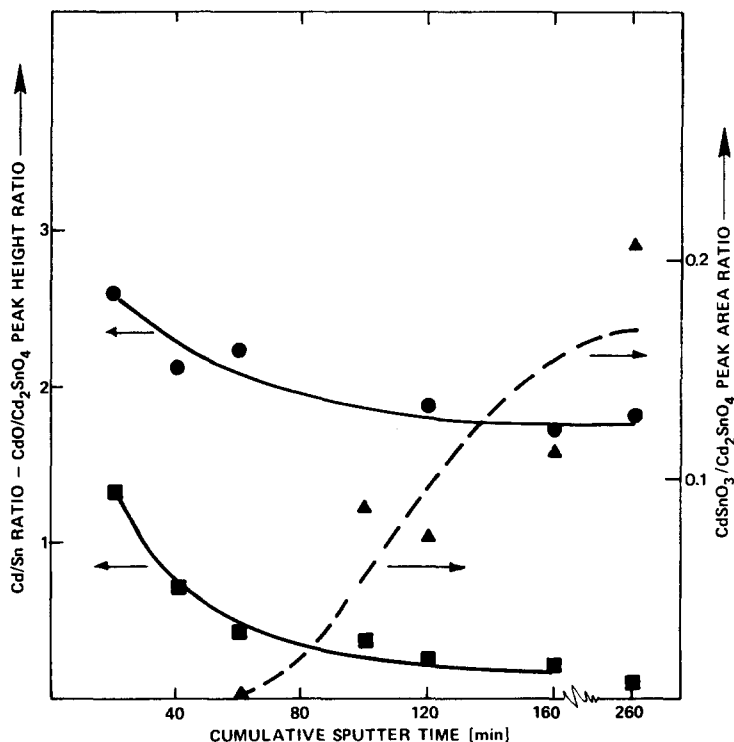


Fig. 4. The initial change of cadmium stannate film compositions during reactive sputtering from a 2Cd:1Sn target: ●, Cd:Sn ratio; ■, CdO:Cd<sub>2</sub>SnO<sub>4</sub> peak height ratio; ▲, CdSnO<sub>3</sub>:Cd<sub>2</sub>SnO<sub>4</sub> peak area ratio.

For the as-sputtered samples the X-ray diffraction patterns showed a small concentration of CdO and some CdSnO<sub>3</sub>. The patterns did not change until 700 °C except for a decrease of the CdO shoulder. Obvious structural changes occurred at 750 °C, leaving only feeble Cd<sub>2</sub>SnO<sub>4</sub> lines. At the same time CdSnO<sub>3</sub> increased in intensity and SnO<sub>2</sub> was formed.

The dependence of the film properties on heat treatment was followed qualitatively by all the sputtered Cd<sub>2</sub>SnO<sub>4</sub> films but quantitative differences were observed in samples prepared under different deposition conditions. Films sputtered from Cd<sub>2</sub>SnO<sub>4</sub> targets at high negative substrate bias (containing no CdO) were stable up to 800 °C. Also, the optimum  $T_H$  at which the lowest sheet resistivities occurred was not always at 650–670 °C but could be as high as 700 °C for films grown on heated substrates. In films prepared from Cd<sub>2</sub>SnO<sub>4</sub> targets on heated



substrates ( $600^\circ\text{C}$ , floating potential) the decrease of the  $\text{CdO}$  phase with  $T_H$  was more pronounced than in reactively sputtered films. The highest electrical conductivity  $\sigma$  (lowest sheet resistivity) coincided with the disappearance of the  $\text{CdO}$  shoulder in the XRD patterns but only when the films were heat treated under Ar–CdS conditions. Films heat treated in argon only always had lower conductivities and  $\text{CdO}$  was still present at the conductivity maximum. Cadmium oxide disappeared from these films at higher  $T_H$  ( $\approx 750^\circ\text{C}$ , see Fig. 2) where  $\sigma$  had already passed its maximum.

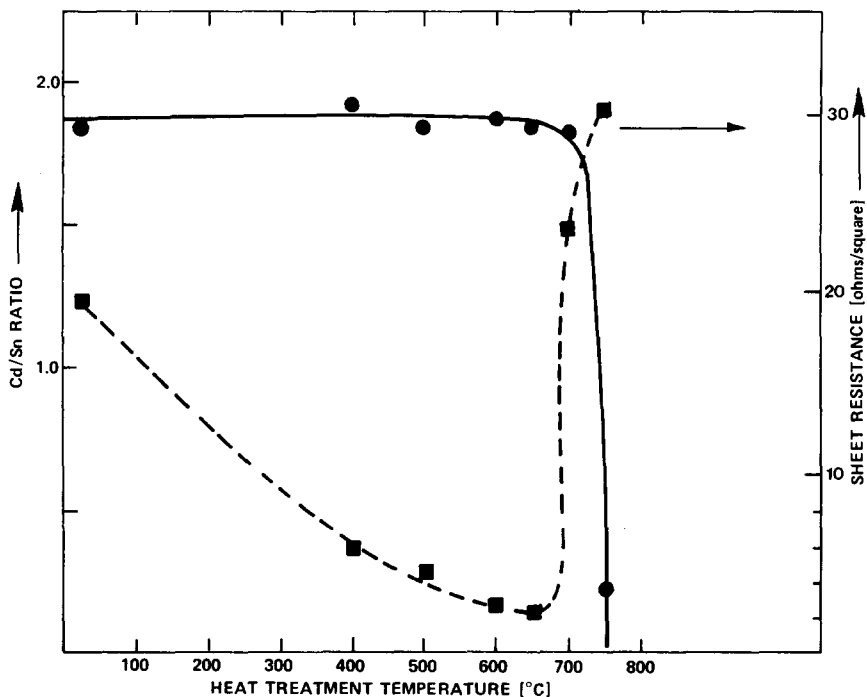


Fig. 5. The electrical sheet resistance (■) and the Cd:Sn ratio (●) of reactively sputtered cadmium stannate films as a function of heat treatment temperature under Ar–CdS conditions.

The above investigations show that the only obvious structural or compositional change accompanying the improvement of the transparent electrode properties of the sputtered  $\text{Cd}_2\text{SnO}_4$  films after heat treatment is a decreasing  $\text{CdO}$  content. The results are not sufficient to identify the underlying mechanism unambiguously. One possible explanation is based on the assumption that at least part of the cadmium dissociates from the  $\text{CdO}$  and diffuses into the  $\text{Cd}_2\text{SnO}_4$  lattice to form interstitial donors. This assumption is supported by an observed increase in lattice constant\* from  $9.167 \text{ \AA}$  for as-sputtered films (Cd–Sn target) to  $9.189 \text{ \AA}$  after heat treatment under Ar–CdS conditions at optimum  $T_H$ . The creation of oxygen vacancies during heat treatment has also to be taken into consideration, however (see Fig. 6 and ref. 3).

\* The lattice constants of sputtered films depend to a certain degree on the deposition conditions but are always larger than those found in fused samples<sup>11</sup>.

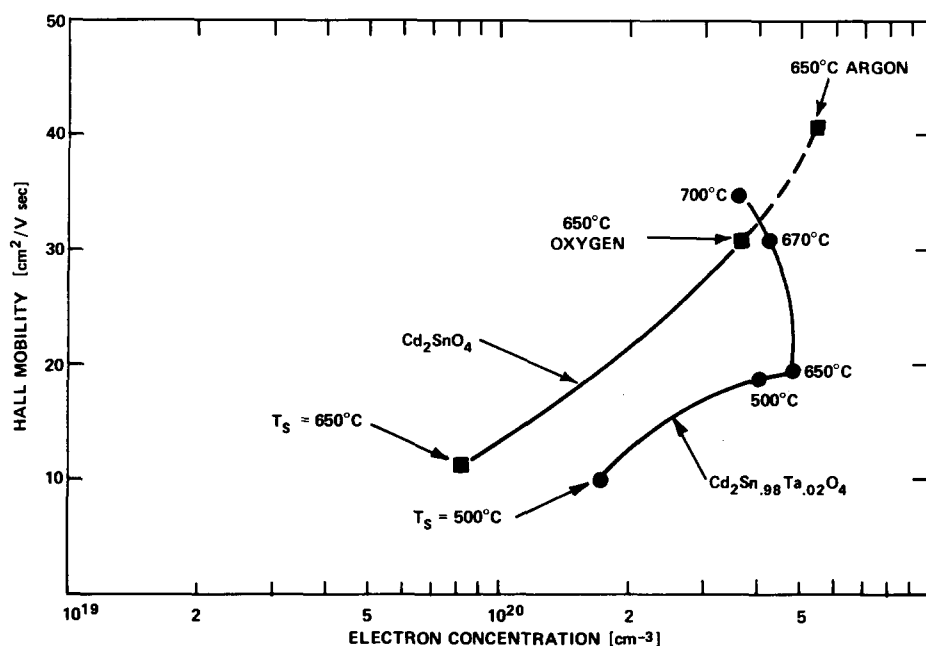


Fig. 6. The Hall mobility as a function of electron concentration (measured at room temperature); the temperature values at the data points indicate the heat treatment temperatures to which samples were exposed before each Hall measurement;  $T_s$  is the substrate temperature during sputter deposition: ■,  $\text{Cd}_2\text{SnO}_4$  film first heat treated in oxygen and then, after the Hall measurement, heat treated in argon; ●, tantalum-doped film heat treated in argon only.

#### 4. ELECTRICAL PROPERTIES

The electrical conductivity  $\sigma$  and optical absorption  $\alpha$  are the basic materials parameters that determine the figure of merit of a transparent conductor<sup>13</sup>. The ratio  $\sigma/\alpha$  should be maximized for the highest figures of merit. Although large conductivities can be obtained by aiming for high free-carrier concentrations  $N$  and high mobilities  $\mu$ , increased mobilities are preferred in order to avoid excessive free-carrier absorption.

Control of  $N$  and  $\mu$  can be accomplished by optimizing the conditions for film growth and by doping. Combining heat treatment (see Section 3.3) with optimized sputter deposition resulted in conductivities as high as  $6700 \Omega^{-1} \text{ cm}^{-1}$ . These values of  $\sigma$  were achieved by sputtering from  $\text{Cd}_2\text{SnO}_4$  ceramic targets onto heated substrates ( $500$ – $600^\circ\text{C}$ ) at a deposition rate of  $150$ – $200 \text{ \AA min}^{-1}$ ; no dopants were intentionally added to the targets. Under these conditions the conductivities of most samples were in the  $5500$ – $6700 \Omega^{-1} \text{ cm}^{-1}$  range. Film preparation under more economical conditions (plasma heating) led to somewhat lower conductivities. When the substrate surface was heated only by the r.f. plasma ( $300 \text{ \AA min}^{-1}$  deposition rate from  $\text{Cd}_2\text{SnO}_4$  targets) the observed values of  $\sigma$  were in the  $5000$ – $6000 \Omega^{-1} \text{ cm}^{-1}$  range. Under the same deposition conditions the  $\sigma$  range was  $4500$ – $5800 \Omega^{-1} \text{ cm}^{-1}$  when the  $\text{Cd}_2\text{SnO}_4$  targets were replaced by Cd–Sn alloy targets.

The conductivity spread was determined in each case from at least 10 samples with 90% falling within the quoted range.

Hall measurements were made to obtain additional information on the basic electrical properties of the sputtered cadmium stannate films. The Hall effect was always measured at room temperature after film deposition and then after heat treatments at progressively increasing temperatures in argon. The effect of heat treatment on the Hall mobility  $\mu$  and electron concentration  $N$  is shown in Fig. 7 for three samples sputtered at different substrate temperatures  $T_s$ . The points marked  $T_s$  were measured immediately after deposition but before heat treatment and show that the initial  $N$  increases with  $T_s$  as would be expected when oxygen vacancies or interstitial cadmium are the donor centers. The film prepared at  $T_s = 300^\circ\text{C}$  was considered to be mostly amorphous since its XRD pattern consisted of only one weak  $\text{Cd}_2\text{SnO}_4$  line. This sample as well as all the other amorphous films measured became highly resistive at an annealing temperature of  $550^\circ\text{C}$  and a Hall voltage could not be detected.

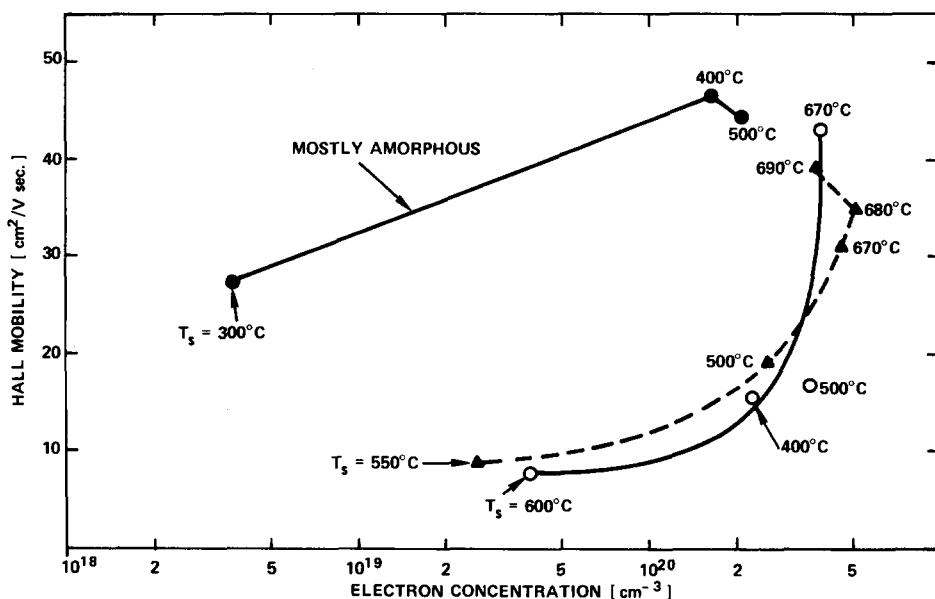


Fig. 7. The Hall mobility as a function of electron concentration (measured at room temperature) for three  $\text{Cd}_2\text{SnO}_4$  films; the temperature values indicate the heat treatment temperatures to which samples were exposed before each Hall measurement;  $T_s$  is the substrate temperature during sputter deposition from a  $\text{Cd}_2\text{SnO}_4$  ceramic target.

The unexpected feature of all three samples in Fig. 7 is an increase of  $\mu$  with  $N$  which contradicts semiconductor theory for homogeneous samples with high carrier concentrations<sup>14</sup>. It therefore appears likely that the electrical properties of these films up to fairly high heat treatment temperatures do not reflect the bulk properties of  $\text{Cd}_2\text{SnO}_4$  but are largely determined by their multiphase composition. Figure 7 indicates that only after heat treatment at high temperatures ( $680^\circ\text{C}$  for the

crystalline films, 400 °C for the amorphous films) does the expected  $\mu$  versus  $N$  relationship exist. In samples heat treated at lower temperatures secondary phases along the grain boundaries or the grain boundaries themselves are suspected of influencing the mobilities significantly. Lower Hall mobilities were shown to result from specimen inhomogeneities when the grains of the main phase were separated by thin layers of a secondary phase<sup>15</sup>. Additional evidence was provided by the higher mobilities found in amorphous films where grain boundaries and secondary phases were less distinct or completely absent. The exact mechanism determining the mobilities at lower  $N$  cannot be ascertained from the above data. Hall measurements over a wide temperature range are required and these data have not yet been obtained.

Figure 7 also supports the assumption that oxygen vacancies are not the only donor centers. The indicated decrease of  $N$  at high annealing temperatures requires the existence of a second species, for instance, the proposed interstitial cadmium which at high temperatures is likely to diffuse out of the  $\text{Cd}_2\text{SnO}_4$ . Indeed, mass spectrometric analysis shows that cadmium and cadmium-oxygen species left the film samples. Furthermore, when sputtered cadmium stannate films were heat treated in pure oxygen instead of argon the  $\mu$  versus  $N$  dependence was similar. This is shown in Fig. 6 by the  $\text{Cd}_2\text{SnO}_4$  curve for which the sample was first heat treated at 650 °C in oxygen and then, after the Hall measurement, at the same temperature in argon. Heat treatment in argon caused an additional increase in  $\mu$  and  $N$ , presumably owing to the formation of oxygen vacancies.

Heat treatment under Ar-CdS led to a  $\mu$  versus  $N$  dependence similar to that for heat treatment in argon alone; however, the maximum electron concentrations reached  $10^{21} \text{ cm}^{-3}$  without a significant reduction in  $\mu$ , resulting in conductivities approximately twice as high as in argon-annealed films. The cause of this improvement is not known but it seems to be connected with the presence of sulfur since a similar less pronounced effect was observed after heat treatment in  $\text{H}_2\text{S}$  while the presence of  $\text{Cd}_2\text{SnO}_4$  powder or  $\text{CdO}$  did not improve the conductivity.

The influence of different doping elements on the electrical properties of  $\text{Cd}_2\text{SnO}_4$  was investigated. Doped  $\text{Cd}_2\text{SnO}_4$  was first prepared in powder form and the electrical conductivity was measured on pressed pellets. Subsequently targets were made by the settling technique. Indium was found to be a donor in powder samples if it was substituted for cadmium<sup>7</sup>, e.g.  $\text{Cd}_{1.98}\text{In}_{0.02}\text{SnO}_4$ . The same was true for antimony and tantalum (on tin sites). Powder data from the remaining specimens containing substitutional dopants (titanium, zirconium, vanadium, niobium, molybdenum, tungsten, rhenium, copper, silver, phosphorus, bismuth, thallium) were ambiguous and doping action could not be ascertained; p-type conductivity was never observed. In sputtered films only tantalum indicated donor properties. The  $\mu$  versus  $N$  dependence of a film with nominal composition  $\text{Cd}_2\text{Sn}_{0.98}\text{Ta}_{0.02}\text{O}_4$  is shown in Fig. 6. This film was prepared at 500 °C substrate temperature and, if undoped, should have had a free-electron concentration of nearly  $10^{19} \text{ cm}^{-3}$  (Fig. 7). The measured electron concentration before heat treatment was  $1.7 \times 10^{20} \text{ cm}^{-3}$  which comes close to the value  $2.2 \times 10^{20} \text{ cm}^{-3}$  expected if each tantalum atom donates one free electron. Higher electron concentrations through increased tantalum doping could not be achieved since the solubility limit is near 2 at.% tantalum.

## 5. OPTICAL PROPERTIES

The optical properties of conducting  $\text{Cd}_2\text{SnO}_4$  beyond the fundamental absorption edge are primarily determined by free-electron effects. Free-carrier absorption controls the visible and infrared absorption while plasma oscillations are responsible for high infrared reflectivities<sup>16</sup>. Figure 8 shows an example of the transmission curves for two films with equal sheet resistances but with different electrical conductivities owing to their different electron concentrations. The expected lower infrared transmission of sample A caused by a stronger free-carrier absorption is clearly indicated. The higher visible transmission of A results from its smaller film thickness ( $1.3\ \mu\text{m}$  compared with  $3.0\ \mu\text{m}$  for B). However, the edge shift towards shorter wavelengths is caused only in part by the reduced film thickness; the Burstein effect also contributes to this shift<sup>3</sup>.

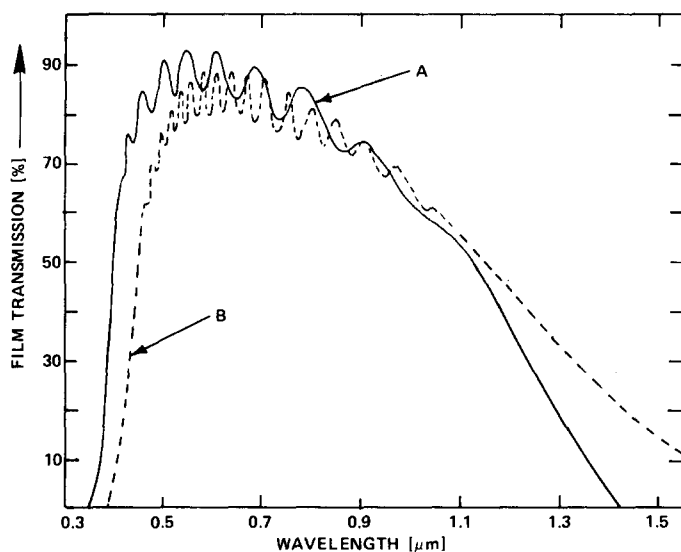


Fig. 8. The optical transmission of two  $\text{Cd}_2\text{SnO}_4$  films of equal sheet resistances but different electrical conductivities (blank substrate in the reference beam): sample A,  $1.36\ \Omega/\square$ ,  $5700\ \Omega^{-1}\text{cm}^{-1}$ ; sample B,  $1.34\ \Omega/\square$ ,  $2500\ \Omega^{-1}\text{cm}^{-1}$ .

We attempted to use Drude's theory to calculate from our transmission, reflection and Hall measurements the optical dielectric constant<sup>17</sup> and the effective mass<sup>18</sup> of cadmium stannate. The numerical values obtained for both constants were found to scatter excessively even for samples with equal free-electron concentrations. The origin of these discrepancies has not yet been identified but the presence of varying amounts of secondary phases in the film samples may be a major factor.

Another set of observations not yet fully understood is a large shift of the fundamental optical absorption edge towards shorter wavelengths with increasing electron concentration. The band edge shifts from approximately 2.1 eV for films sputtered in oxygen to more than 2.9 eV after heat treatment; this shift was first

observed in amorphous samples<sup>3</sup>. Since the shift is accompanied by an increase of almost three orders of magnitude in the free-electron concentration it was attributed to the Burstein effect. Assigning the full shift to the Burstein effect in  $\text{Cd}_2\text{SnO}_4$  led to an abnormally low effective mass (0.04) at the bottom of the conduction band. In view of the multiphase composition of the sputtered  $\text{Cd}_2\text{SnO}_4$  films discussed earlier in this paper it now appears more likely that the observed shift is composed of contributions from  $\text{Cd}_2\text{SnO}_4$  and  $\text{CdO}$ ;  $\text{CdSnO}_3$  has not been sufficiently investigated to determine whether it also shows a Burstein effect. The Burstein effect in  $\text{CdO}$  is well established<sup>19, 20</sup> and could account for the long wavelength portion of the total shift in the sputtered cadmium stannate films. With this interpretation, the band gap value of low conductivity  $\text{Cd}_2\text{SnO}_4$  films is in doubt and its determination will have to wait until  $\text{CdO}$ -free samples with low electron concentrations become available. Thus far, films free of  $\text{CdO}$  have only been obtained either by applying a high negative bias voltage to the substrate or by heat treatment under Ar-CdS conditions. In both cases the samples had electron concentrations higher than  $10^{20} \text{ cm}^{-3}$ .

It should be added that single-phase orthorhombic  $\text{Cd}_2\text{SnO}_4$  powders also show an absorption edge shift with increasing electrical conductivity<sup>3</sup> indicating that there is indeed a Burstein effect in  $\text{Cd}_2\text{SnO}_4$ . However, in single-phase powders the shift is much smaller than in sputtered films and extends from only 2.34 eV to 2.76 eV. These absorption edge values do not necessarily apply to thin films since they have a different crystal structure.

## 6. CONCLUSIONS

Thin films of  $\text{Cd}_2\text{SnO}_4$  prepared by r.f. sputtering were found to contain small concentrations of  $\text{CdO}$  and/or  $\text{CdSnO}_3$ . The presence of either phase affects the electrical and optical film properties and masks the intrinsic materials parameters of  $\text{Cd}_2\text{SnO}_4$ .

Despite the difficulties encountered in preparing single-phase films, it has been demonstrated<sup>1, 2</sup> that properly treated cadmium stannate coatings are excellent transparent conductors suitable for a multitude of applications. For instance, films for high quality display electrodes (Fig. 9) can easily be prepared and require only short deposition times; an economical manufacturing technique can be foreseen if sputtering and heat treatment are integrated into one continuous process. The economics would improve significantly if conditions were found for the formation of single-phase  $\text{Cd}_2\text{SnO}_4$  films. If this were the case post-deposition heat treatment might be unnecessary and even more attractive transparent electrode properties could be expected as a result of potentially higher electron mobilities.

## ACKNOWLEDGMENT

The work reported in this paper was supported in part by the Air Force Materials Laboratory and the National Science Foundation (Research Applied to National Needs).

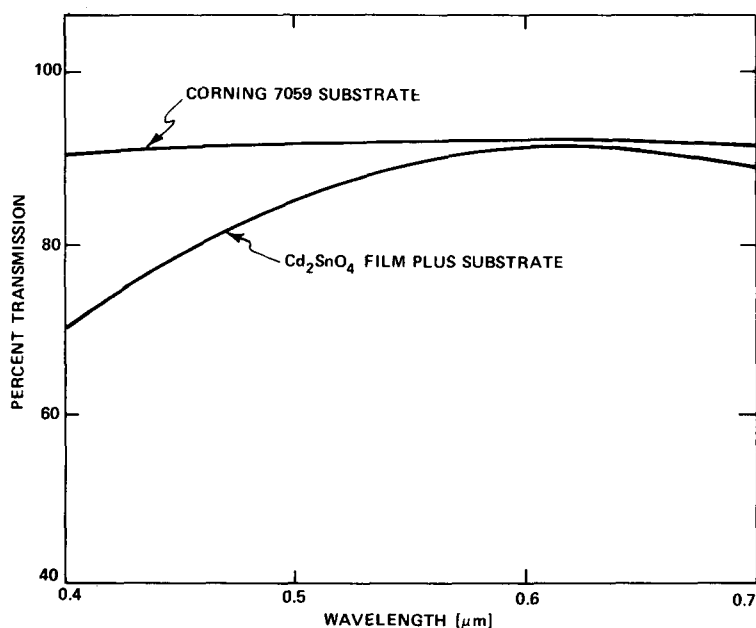


Fig. 9. The visible optical transmission of a  $\text{Cd}_2\text{SnO}_4$  electrode for display devices: deposition time, 5 min; Cd-Sn alloy target; sheet resistance,  $18 \Omega/\square$ ; luminous transmittance, 88.9%.

#### REFERENCES

- 1 G. Haacke, *Appl. Phys. Lett.*, **28** (1976) 622.
- 2 G. Haacke, *J. Appl. Phys.*, **47** (1976) 4086.
- 3 A. J. Nozik, *Phys. Rev., Sect. B*, **6** (1972) 453.
- 4 G. Haacke, *Report NSF/RANN/SE/GI-39539/PR/74/1*, 1974.
- 5 G. K. Wehner, C. E. KenKnight and D. Rosenberg, *Planet. Space Sci.*, **11** (1963) 1257.
- 6 G. Haacke, H. Ando and W. E. Mealmaker, *J. Electrochem. Soc.*, **124** (1977) 1923.
- 7 Air Force Materials Laboratory, *Tech. Rep. AFML-TR-75-21*, 1975.
- 8 M. Trömel, *Z. Anorg. Allg. Chem.*, **371** (1969) 237.
- 9 L. I. Maissel and P. M. Schaible, *J. Appl. Phys.*, **36** (1965) 237.
- 10 M. L. Tarng and G. K. Wehner, *J. Appl. Phys.*, **42** (1971) 2449.
- 11 L. A. Siegel, *J. Appl. Crystallogr.*, **11** (1978) 284.
- 12 E. Gillam, *J. Phys. Chem. Solids*, **11** (1959) 55.
- 13 G. Haacke, *Annu. Rev. Mater. Sci.*, **7** (1977) 73.
- 14 C. Hilsum and A. C. Rose-Innes, *Semiconducting III-V Compounds*, Pergamon, New York, 1961.
- 15 J. Volger, *Phys. Rev.*, **79** (1950) 1023.
- 16 G. Haacke, *Appl. Phys. Lett.*, **30** (1977) 380.
- 17 H. Finkenrath and M. von Ortenberg, *Z. Angew. Phys.*, **23** (1967) 323.
- 18 W. G. Spitzer and J. M. Whelan, *Phys. Rev.*, **114** (1959) 59.
- 19 J. Stuke, *Z. Phys.*, **137** (1954) 401.
- 20 H. Finkenrath, *Z. Phys.*, **159** (1960) 112.